Chaos in Neural and Gene Networks with Hard Switching

R. Edwards

Department of Mathematics and Statistics

University of Victoria

P.O.Box 3045, STN CSC

Victoria, BC, Canada V8W 3P4

E-mail: edwards@math.uvic.ca

31 Aug. 2001

Abstract

Although there are ways of demonstrating the existence of chaotic dynamics on certain sets in nonlinear systems of ODEs, it is often very difficult to prove that such sets are attracting. In the context of neural networks and networks that model gene regulation or chemical kinetics, the use of a hard switching nonlinearity or Heaviside step function response for each network unit has been shown to give considerable analytic leverage. These 'Glass networks', named after their originator, have been shown to have an interesting range of possible dynamics in 4 or more dimensions, and a number of attempts have been made to pin down chaotic dynamics in particular examples. However, the existence of a chaotic attractor has never been proven in any such network, despite demonstration of the existence of transverse homoclinic points and sets on which the dynamics are homeomorphic to shifts of finite type. The problem has been that the sets supporting chaotic dynamics need not be attracting, so that long, stable periodic solutions remained a possibility. Here we present a method of proof that the dynamics on an attractor in a particular network is aperiodic and we demonstrate its application in three examples. The method uses matrix theoretic techniques which are sufficient to prove non-existence of stable periodic orbits in many chaotic networks particularly in 4 dimensions, though they may not be sufficient for every such network.

Keywords: Neural networks, limit cycles, chaos, Glass networks, attractor, aperiodicity

1 Introduction

There has been an interest for some time now in the possibility of chaotic dynamics in neural networks, though its rôle remains controversial (e.g. [1, 2]) and its presence in real biological neural networks even more so [3]. Whatever its potential function, the approach to identifying chaos in network models has typically been numerical integration and sometimes indirect tests such as for positive Lyapunov exponents in time series generated by the network equations (e.g. [4, 5]). Analytic proof of stable (attracting) chaotic dynamics in neural network equations has so far been rare and dependent on special constructions [6, 7, 8, 2, 9]. In this paper we describe a general approach to proving the existence of attractors with at least aperiodic dynamics in a broad class of networks, and demonstrate it with some examples. We do not address here the notorious problem of identifying chaos in data obtained from physiological neural systems [3].

Neural network models are highly nonlinear, principally due to the ubiquitous sigmoidal functions that occur at all scales of description, from electrochemical models of membrane activity to coarse-scale models of abstracted neural activity in large networks, but also due in some cases to quadratic or higher order product terms. These nonlinearities and the large number of dimensions make it difficult to show analytically that a network has any particular dynamical behaviour. The existence of a Lyapunov functional for additive (Cohen-Grossberg-Hopfield) networks with symetric connections is an exceptional case that allows a rather beautiful proof that all trajectories converge to a fixed point [10, 11, 12]. In other contexts, particularly in attempts to deal with questions about physiological networks, fixed points are not necessarily expected and oscillation is ubiquitous. Proof of the existence of stable limit cycles in neural networks is generally much more difficult than proof of the existence of stable fixed points. Proof of the existence of stable chaotic dynamics,

or any kind of aperiodic dynamics, is considerably more difficult still. Existing work on these lines seems to rely on constructions involving known chaotic equations or systems. Networks have been built, for example, out of chaotic components such as discrete time quadratic maps (e.g. [8, 2]). Wang [7] proved the existence of stable chaotic behaviour in a family of simple discrete-time two-neuron networks, but again the construction amounted to choosing an excitatory and an inhibitory response function so that together they act as a unimodel one-dimensional map (like the logistic map) known to be chaotic, an idea also exploited by Priesol *et al.* [13]. Lapedes and Farber [6] raised the idea of training a network (in their case a multi-layer perceptron network with backpropogation) to predict the dynamics of a known chaotic equation such as the logistic map or the Mackey-Glass equation. Here again, although a network with stable chaotic dynamics is the result, data from a known chaotic equation must be used to train the network in the first place.

Despite the general intractability of highly nonlinear systems like neural networks, considerable analysis, particularly for limit cycles, has proven to be possible in networks in which all interactions take the form of the 'high gain' limit of sigmoidal interaction — a step function [14, 15, 16]. Networks with steep sigmoids display switching behaviour as variables cross their thresholds. The high-gain limit could be called 'hard switching'. There is good evidence that dynamical behaviour of networks with sufficiently steep sigmoid interactions are qualitatively the same as the networks obtained by taking the limiting step function interactions [17, 4, 5], and at least some analytic results along these lines [18]. The hard-switching limit puts us into the context of what have been called 'Glass networks' after their originator [21]. The current work presents a method by which the existence of attracting aperiodic dynamics can be proven analytically at least in some networks of this type.

Glass networks [16] are sytems of ordinary differential equations in which all interactions between variables are of the hard switching type. They have been studied

both in the context of neural networks and of gene regulatory and other biochemical networks (and are to be contrasted with the discrete time Boolean networks whose theory has been developed by Kauffman [19]). The occurrence of complex dynamics in Glass networks has been discussed in a number of papers [4, 5, 20, 21, 16, 22, 23]. Very complicated periodic orbits have been shown to exist in Glass networks of as few as 4 interacting elements [22, 24] and evidence has been found for chaotic dynamics, discussed further in Section 3 below. Sets on which the dynamics are chaotic have been shown to exist, but it has not been shown that these sets are attracting. The possibility has always been open that stable long periodic solutions exist in these networks despite the apparent irregularity of numerically computed solutions. Here, we present a proof that this is not the case in three example networks, including the one studied by Mestl et al. [20]. This is the first complete proof of the existence of attracting aperiodic dynamics in any Glass network.

Although the approach is indirect, in that it focusses on proving the non-existence of stable periodic orbits (or stable fixed points) in some trapping (invariant) region, and thus allows only the conclusion that the attractor in this region must be aperiodic, when this result is combined with the previous work indicating the existence of sets supporting chaotic dynamics, it seems clear that the dynamics on the attractor is indeed chaotic, rather than having some other kind of aperiodicity. Quasiperiodicity is possible in these networks but is a special behaviour depending on non-interaction of units involved in periodic orbits with non-commensurable periods, which is not the situation in any of the examples studied here or in any of the above-cited references.

2 Background

Glass networks can be expressed in the form

$$\dot{y_i} = -y_i + F_i(\tilde{\mathbf{y}}) \,, \quad \tilde{\mathbf{y}} = (\tilde{y}_1, \tilde{y}_2, \ldots, \tilde{y}_n)' \,, \quad i = 1, \ldots, n \,, \tag{1}$$

where

$$\tilde{y}_i = \begin{cases} 0 & \text{if } y_i < 0 \\ 1 & \text{if } y_i > 0 \end{cases} , \tag{2}$$

and the prime ($'$) denotes matrix transposition. Additive neural networks with hard switching fall into this class. In that case,

$$F_i(\tilde{\mathbf{y}}) = W\tilde{\mathbf{y}} - \tau \, , \tag{3}$$

where W is the connection matrix, and τ is the vector of thresholds. Other neural network frameworks are not additive and may for example have quadratic terms. As long as all such interaction terms are passed through the nonlinearity, and if we take the hard switching nonlinearity (Heaviside step function), then these other neural networks still clearly fit into the framework of Equations 1 and 2. Note that thresholds at non-zero values and outputs of the switching function other than 0 and 1, can be accommodated into the above framework by transformation of variables even if these values are non-uniform. Non-uniform decay rates also do not present a major problem and the theory for Glass networks can be extended to cover them. While Equation 2 does not define $\tilde{y}_i$ when $y_i = 0$, trajectories in almost all cases can be extended in an unambiguous way to their limiting value as $y_i \to 0$ from either side. The only exceptions occur when a trajectory passes through a point where two or more variables are zero simultaneously in which case there may or may not be an unambiguous continuation, but such trajectories form a set of measure zero in $\mathbf{R}^n$ and we do not consider them further.

Solutions to these equations consist of continuous, piecewise-linear trajectories with corners where orthant boundaries are crossed in phase space. Within an orthant specified by sign structure $\tilde{\mathbf{y}}$, a trajectory is a straight line directed towards a focal point, $\mathbf{f} = \mathbf{F}(\tilde{\mathbf{y}})$. If the focal point for a particular orthant lies within that orthant, then it is a fixed point of the dynamics and any trajectory entering this orthant approaches the fixed point asymptotically. If there is no self-input in the network,

i.e., if for all i, F_i does not depend on y_i, then the only other possibility is that a trajectory consists of a continuing sequence of piecewise-linear segments, which can be specified by the crossing points on the orthant boundaries. Throughout this paper we will assume that there is no self-input in our networks, though allowing self-input does not invalidate our results as long as our trajectories stay away from orthant boundaries that cannot be crossed ('black' and 'white' walls in the terminology used in Reference [20]). We will also only be interested in trajectories that do not enter an orthant containing its own focal point, in which case no more crossings occur.

Thus, trajectories for an n-dimensional network (n-net) may be specified by a discrete mapping on the $(n-1)$-dimensional boundaries. These are fractional linear mappings of the form

$$\mathbf{y}^{(k+1)} = M^{(k)}\mathbf{y}^{(k)} = \frac{B^{(k)}\mathbf{y}^{(k)}}{1 + \langle \psi^{(k)}, \mathbf{y}^{(k)} \rangle}\,, \tag{4}$$

where

$$B^{(k)} = I - \frac{\mathbf{f}^{(k)}\mathbf{e}_j'}{f_j^{(k)}}\,, \quad \psi^{(k)} = \frac{-\mathbf{e}_j}{f_j^{(k)}}\,, \tag{5}$$

j is the index of the variable that switches on exiting the k^{th} orthant along the trajectory, $\mathbf{e}_j$ denotes the standard basis vector in $\mathbf{R}^n$, and the angle brackets denote the Euclidean inner product ($\langle \psi, \mathbf{y} \rangle = \psi'\mathbf{y}$). This mapping can be reduced to $n-1$ dimensions by removing the i^{th} column and j^{th} row of the matrix $B^{(k)}$ and the i^{th} element of all the vectors, where i is the index of the variable that switched on entry to the orthant.

Fractional linear mappings of this form are closed under composition. Thus, if a trajectory cycles from a given orthant boundary back to the same boundary, that cycle corresponds to a mapping

$$M\mathbf{x} = \frac{A\mathbf{x}}{1 + \langle \phi, \mathbf{x} \rangle}\,, \tag{6}$$

where $A \in \mathbf{R}^{(n-1)\times(n-1)}$ and $\phi \in \mathbf{R}^{n-1}$. Here and throughout this paper we use

$$\mathbf{x} = \mathbf{y}|_{(i)}\,,$$

the vector $\mathbf{y}$ reduced to dimension $n-1$ by removing the i^{th} variable, which is zero on the boundary on which the cycle is defined. We denote this starting boundary for a cycle $\mathcal{O}^{(0)}$.

Whenever it is possible to exit from an orthant by multiple boundaries (i.e. more than one variable may reach zero first) only part of a given entry boundary to the orthant will map to each possible exit boundary. Extrapolating, only part of a boundary will contain trajectories that follow a given sequence of orthants and return to that boundary, in general. This domain of definition for a cycle map may in fact be empty, in which case no trajectories follow that cycle, or may be the entire starting boundary, $\mathcal{O}^{(0)}$. In general, it is a subset of $\mathcal{O}^{(0)}$, defined by a set of linear inequalities, and we call it the returning cone, C, for the map. It can be calculated as follows:

$$C = \{\mathbf{y} \in \mathcal{O}^{(0)} | R\mathbf{y} \geq 0\}, \tag{7}$$

where R is a matrix with one row for each alternate exit variable around the cycle, being the row vector

$$R_{i,\cdot} = -\frac{\mathbf{e}_i'}{f_i^{(k)}} B^{(k)} B^{(k-1)} \dots B^{(0)} \tag{8}$$

in each case.

As we will make considerable use of cones, we briefly give a few definitions here [25, chapter 1]. For a set $S \subseteq \mathbf{R}^n$, *the set generated by* S is the set of finite nonnegative linear combinations of elements of S:

$$S^G = \{\sum_{i=1}^{m} c_i x_i, \text{ for some } c_i \geq 0, x_i \in S, m \text{ finite}\}.$$

A set K is a *cone* if $K = K^G$, so for any S, S^G is clearly a cone. Note that this definition implies that all cones are convex. Sometimes, the above is taken to define a *convex cone*, while a *cone* is defined simply as a set K for which $cK \subseteq K, \forall c \geq 0$ [26]. In any case, we are concerned mainly with convex cones, so the distinction matters little in our context. K is a proper cone if it is convex, closed, solid ($\text{int}(k) \neq \emptyset$) and

pointed ($K \cap (-K) = \{\mathbf{0}\}$). *Extremal* vectors of a proper cone are those required (up to nonnegative multiples) to generate it. A *polyhedral cone* is one that can be generated by a finite set S. For example, the returning cone, C, above is polyhedral, generated by intersections of the $(n-1)$-dimensional hyperplanes in the rows of $R\mathbf{y} = 0$ and the boundaries of $\mathcal{O}^{(0)}$.

Now we state without proof results on the existence and stability of periodic orbits in Glass networks [16].

Proposition 1 *Trajectories starting on the same ray through the origin remain on the same ray through the origin under the discrete mapping. Furthermore, trajectories from points on the same ray converge under the discrete mapping as* $t \to \infty$.

Note that it is possible for infinite iteration of the mapping to occur in finite time, when some variables are spiralling in to zero. In this case, coordinates corresponding to other variables will not have had time to converge and the infinite sequence of iterations of the map does not describe the trajectory for all time. However, the variables that have reached zero should then remain zero until some other variable switches and a new sequence commences, unless the multiplicity of variables at zero makes continuation ambiguous. If continuation is possible, then, trajectories starting from points on the same ray continue to converge (see Reference [16]).

Proposition 2 *The fractional linear map of Equation 6 maps straight lines to straight lines, and in general linear subspaces to linear subspaces.*

Proposition 3 *If* $\mathbf{v}$ *is an eigenvector of* A *in Equation 6, corresponding to eigenvalue* $\lambda \neq 0$*, such that* $\langle \phi, \mathbf{v} \rangle \neq 0$*, then*

$$\mathbf{y}^* = \frac{(\lambda - 1)\mathbf{v}}{\langle \phi, \mathbf{v} \rangle} \tag{9}$$

is a fixed point of M *and there is no other non-zero fixed point in the span of* $\mathbf{v}$.

Proposition 4 *If the map M for a cycle has a fixed point in C, then it lies on an eigenvector of A with eigenvalue $\lambda > 1$. Conversely, if A has an eigenvector in C with eigenvalue $\lambda > 1$, then M has a fixed point in C.*

Proposition 5 *A fixed point $\mathbf{y}_i^*$ of the discrete map (Equation 6) is asymptotically stable if the corresponding eigenvalue λ_i of the matrix A is the unique dominant one ($\lambda_i > |\lambda_j|, j \neq i$); it is neutrally stable if λ_i is dominant but $\lambda_i = |\lambda_j|$ for some $j \neq i$; and it is unstable otherwise.*

Note that for any periodic orbit, $\langle \phi, \mathbf{v} \rangle > 0$ [16], because the denominator of the mapping (Equation 6) is the exponential of the period of the orbit. It may occur that $\langle \phi, \mathbf{v} \rangle = 0$ for a fixed point, $\mathbf{v}$, of the mapping. In that case, the "period" of the limiting orbit is 0, so that $\mathbf{v}$ is actually a stable fixed point. It must then be 0 in all variables that switch in the cycle. Trajectories spiral in to the fixed point. Note that in this case, $A\mathbf{v} = \mathbf{v}$, which implies that $\mathbf{v}$ is an eigenvector corresponding to eigenvalue 1.

On a given orthant boundary, $\mathcal{O}^{(0)}$, several cycles that return to the same boundary may be possible, each with its own returning cone. For example, we may have $M_A : C_A \to \mathcal{O}^{(0)}$ and $M_B : C_B \to \mathcal{O}^{(0)}$. The image of C_A under M_A may intersect with C_B and *vice versa*. Thus, trajectories may follow a complex sequence of cycles corresponding to repeated composition of M_A and M_B in some order. An example of such a situation occurs in the network studied in Refs. [20, 23]. Numerical investigations of a number of Glass networks of dimension 4 or more have appeared to show very complex sequences of this type. There may also be more than two mappings defined on a boundary as in the example studied in Ref. [16], and in Example 3 below.

3 The question of aperiodic dynamics on attractors

The above-mentioned examples appear to exhibit chaotic dynamics. Mestl *et al.* [20] were able to show that their example network had a trapping region, *i.e.*, a cone on an orthant boundary that was invariant under the Poincaré map consisting of two regions, one on which M_A operated and one on which M_B operated. Each mapping had an unstable fixed point in its part of the trapping region. They showed that the stable and unstable manifolds of these fixed points intersected to produce transverse homoclinic points. This essentially guarantees that there is a set on which the dynamics are chaotic. However, they were not able to show that this set was attracting, and the possibility was left open that there might still be a very long and complicated periodic orbit that was attracting. Edwards *et al.* [23] showed that the symbolic sequences of A's and B's corresponding to trajectories could not contain the sequence BB, although bifurcation as a parameter changed could alter the dynamics to allow this symbolic subsequence.

Another network has been shown to contain a 'golden mean map', with topology homeomorphic to a shift of finite type, similar to the Smale horseshoe, but this only applied on a set that was certainly not itself an attracting set, since the dynamics actually involved many other cycle mappings besides the two that made up the golden mean map [16].

Numerical investigations of example additive networks suggest that dynamics of complicated trajectories are ergodic in the sense that they converge to an invariant distribution of values of each variable. Lewis and Glass [4, 5] showed by numerical simulation that in these examples, the invariant density across many different initial conditions evolved over time to match the invariant density along a single trajectory. This suggests the existence of a nontrivial attractor with sensitive dependence on

initial conditions. Lewis and Glass also calculated Lyapunov exponents for their integrated trajectories and found good evidence for a positive exponent, again suggestive of chaos. The difficulty with these methods is that they rely on numerical integrations and do not constitute a proof. There is no guarantee that the trajectories calculated are not on long transients and have not reached an attractor, that they are not on a very complex periodic orbit or that accumulation of numerical errors is not critical.

While it has seemed virtually certain for some time that these examples do exhibit stable chaotic dynamics, this has not been proven. While long stable periodic orbits seem unlikely in these examples, they have not been ruled out. It should be noted that it is possible, even in networks of only four elements, to have long and complex but stable limit cycles. Even in the class of networks in which the focal point coordinates F_i are all ± 1, 4-nets have been found with stable limit cycles consisting of up to 252 switchings (or linear trajectory segments) [22]. Gedeon has constructed 4-net examples in the general class (arbitrary F_i) with stable limit cycles consisting of arbitrarily many switchings [24]. These results make it unclear whether or not such long periodic attractors exist in the apparently chaotic networks. While negative divergence implies the contraction of phase space and the existence of attractors of dimension $< n$ [16], the question remains: Are attracting aperiodic dynamics possible in Glass networks (aside from obvious but special constructions of quasiperiodic attractors)?

4 Matrices and invariant cones

Proposition 1 implies that the radial component of a cycle map's dynamics can be factored out, unless trajectories converge to the origin. Except in the latter special case, we can ignore the radial component and consider the discrete map (Equation 6) to be essentially a matrix multiplication acting on a ray:

$$M\mathbf{x} = A\mathbf{x}\,, \tag{10}$$

where $\mathbf{x}$ may now be taken to represent an entire ray, rooted at the origin. The scalar division in the fractional linear map only moves a point in or out on the ray. The results outlined in the previous section imply that there is a stable periodic orbit following a given cycle if its matrix, A, has its dominant eigenvalue, λ_1, real and > 1 and the corresponding dominant eigenvector (which must then be real) in its returning cone, C. A stable spiral fixed point is a degenerate case of such a periodic orbit with $\lambda_1 = 1$. Complex cycles, made of compositions of a pair of maps, for example M_A and M_B, can now be considered as a 'word' made up of A's and B's (being in fact a matrix product, as well as a symbolic sequence). In order for such a word, W, to correspond to a stable periodic orbit, the dominant eigenvector of W must lie in its returning cone. This is a statement about the location of the dominant eigenvector of a matrix product. While there is no general result in linear algebra for the location of eigenvectors of a matrix product in terms of the eigenvectors of the individual matrices (they can go anywhere), there *are* results dealing with the location of a dominant eigenvector that we can use, the most obvious being the Perron-Frobenius theorem and generalizations.

A finite-dimensional version of the Krein-Rutman theorem generalizes the Perron-Frobenius theorem from nonnegative matrices to any matrix that leaves a proper cone invariant. We give two versions of this result (adapted from Berman and Plemmons [25, chapter 1]).

Theorem 6 *If $K \in \mathbf{R}^n$ is a proper cone and $AK \subseteq K$, where $A \in \mathbf{R}^{n\times n}$, then the spectral radius, $\rho(A)$, is an eigenvalue and a corresponding eigenvector lies in K.*

Theorem 7 *If $K \in \mathbf{R}^n$ is a proper cone and $A(K - \{\mathbf{0}\}) \subseteq \mathrm{int}K$ (*i.e.*, A is K-positive) then $\rho(A)$ is a simple eigenvalue and its corresponding one-dimensional eigenspace lies in $\mathrm{int}(K \cup (-K)) \cup \{\mathbf{0}\}$.*

It is easy to see that if $AK \subseteq K$ and $BK \subseteq K$, where K is a proper cone, then

not only must eigenvectors corresponding to $\rho(A)$ and $\rho(B)$ lie in K but the same must be true of any matrix W made up of a product of A's and B's in any order, since each consecutive multiplication by A or B maps K into K.

Proposition 8 *Let $(A^*B^*)^*$ be the set of all finite matrix products of A's and B's in any order. If $AK \subseteq K$ and $BK \subseteq K$, where K is a proper cone, then $WK \subseteq K$, $\rho(W)$ is an eigenvalue of W, and a corresponding eigenvector lies in K, for any $W \in (A^*B^*)^*$.*

We wish to argue that no eigenvector corresponding to $\rho(W)$ can lie anywhere other than $K \cup (-K)$. The above result is sufficient as long as $\rho(W)$ is a simple eigenvalue of W. Otherwise, $\rho(W)$ may have an eigenspace of dimension > 1 and the existence of an eigenvector in K is not sufficient to preclude an eigenvector elsewhere. Even if $\rho(A)$ and $\rho(B)$ are simple eigenvalues of A and B, it is not immediate that this is true for every product W. For any W for which $W(K - \{\mathbf{0}\}) \subseteq \text{int}(K)$, however, we can apply Theorem 7.

Proposition 9 *Suppose a union of (solid but not necessarily proper) cones, $T = T_A \cup T_B$, of an orthant boundary, $\mathcal{O}^{(0)}$, is invariant under the network dynamics consisting of two cycle maps, $M_A : T_A \to T$ and $M_B : T_B \to T$. Suppose there exists a proper cone K such that $AK \subseteq K$ and $BK \subseteq K$, and that $(K \cup (-K)) \cap T = \{\mathbf{0}\}$. Then there is no stable periodic orbit through T for any cycle $W \in (A^*B^*)^*$ for which $W(K - \{\mathbf{0}\}) \subseteq \text{int}(K)$.*

Proof: Under the network dynamics, every point $x \in T$ returns to T repeatedly after following either cycle A or B each time. T is a Poincaré section for the Poincaré map,

$$M\mathbf{x} = \begin{cases} M_A\mathbf{x} & \text{if } \mathbf{x} \in T_A \\ M_B\mathbf{x} & \text{if } \mathbf{x} \in T_B \end{cases} . \tag{11}$$

Thus, each point (or ray) in T has a corresponding symbolic sequence in $(A^*B^*)^*$. Suppose now that there is a stable periodic orbit through T. Then this corresponds

to a non-zero fixed point $\mathbf{x} \in T$ of a composite mapping whose matrix is some $W \in (A^*B^*)^*$. By Propositions 4 and 5, $\mathbf{x}$ is a dominant eigenvector of W, and its corresponding eigenvalue is $\rho(W) > 1$. However, since K is a common invariant proper cone for both A and B, any $W \in (A^*B^*)^*$ has a dominant eigenvector in K (and $-K$), by Proposition 8. Furthermore, if $W(K - \{\mathbf{0}\}) \subseteq \text{int}(K)$, then this dominant eigenvector is unique up to scalar multiples, by Theorem 7. This contradicts the assumption that $(K \cup (-K)) \cap T = \{\mathbf{0}\}$, *i.e.*, that the only point in the intersection of T and $K \cup (-K)$ is the origin. $\mathbf{x}$ cannot be in both T and $K \cup (-K)$. ■

Remark 1: The conditions of the theorem are not contradictory. We are supposing that K is invariant for A and B individually. We do not assume that T is invariant for A or B, rather that it is invariant for M which is defined so that A applies on T_A and B applies on T_B. It is entirely possible for this arrangement to occur — see the examples in Section 5.

Remark 2: Note that if $-A$ and B leave a proper cone, K, invariant or map it into its interior then the above theorems apply to $((-A)^*B^*)^*$, and since any $W \in (A^*B^*)^*$ is $\pm$ an element of $((-A)^*B^*)^*$, we have that $\pm\rho(W)$ is an eigenvalue of W and the corresponding eigenvector still lies in $K \cup (-K)$. The same is clearly true if $-B$, rather than B, leaves K invariant.

Remark 3: It is easy to see that a similar result also holds when there are more than two cycles involved, with $T = \bigcup_i T_i$ and $M_i : T_i \to T$ if K is invariant simultaneously for all A_i (the matrix of M_i).

Remark 4: In practice, this result implies that words W that do not map K into its interior, *i.e.*, that map non-zero boundary points to non-zero boundary points of K, have to be checked separately. In each case if $\rho(W)$ is simple or if it is not simple but still no corresponding eigenvector lies in T then there is no stable periodic orbit corresponding to the cycle W.

If trajectories are trapped in a trapping region, T, and no stable limit cycles pass

through T then the only remaining possibilities for the dynamics are convergence to a fixed point or aperiodicity. Convergence to a fixed point other than the origin implies a spiral point on the boundary of $\mathcal{O}^{(0)}$, which is covered as a degenerate case under the results on stable periodic orbits, so the only further check required is for convergence to the origin. (Recall that we have ruled out trajectories ending at a fixed point in the interior of an orthant). There is always an attractor of dimension $< n$, since the flow of these networks (under the condition of no self input) is contracting. From the point of view of the Poincaré map, the determinant of the matrix A in the map is 1 (under the no self input condition) and the denominator of the map is always greater than 1, so volumes contract [16].

The question of convergence to the origin is dealt with by the following proposition.

Proposition 10 *Let $T = T_A \cup T_B$ be a trapping region on an orthant boundary for a network such that cycle maps M_A and M_B are defined on polyhedral cones T_A and T_B respectively. Let A be the matrix in the map M_A (Equation 6) and B be the matrix in M_B. Let $\mathbf{x}_i, i = 1, \ldots, k$ and $\mathbf{y}_i, i = 1, \ldots, m$ be the extremal vectors of cones T_A and T_B respectively with unit L^1 norm. If $||A\mathbf{x}_i||_1 > 1$ for $i = 1, \ldots, k$ and $||B\mathbf{y}_i||_1 > 1$ for $i = 1, \ldots, m$, then no trajectory in T can converge to the origin.*

Proof: Consider one of the unit extremal vectors $\mathbf{x}_i$. Let

$$0 < c < \frac{||A\mathbf{x}_i||_1 - 1}{\phi' \mathbf{x}_i} = c_i^* \,.$$

Then

$$||M_A(c\mathbf{x}_i)||_1 = \frac{||A(c\mathbf{x}_i)||_1}{|1 + \phi'(c\mathbf{x}_i)|} = \frac{c||A\mathbf{x}_i||_1}{1 + c\phi'\mathbf{x}_i}$$

since $1 + \phi'(c\mathbf{x}_i) > 1$ when $\mathbf{x}_i \neq \mathbf{0}$ (see note following Proposition 5). Our assumed range for c implies that

$$1 + c\phi'\mathbf{x}_i < ||A\mathbf{x}_i||_1 \,,$$

so

$$||M_A(c\mathbf{x}_i)||_1 > c = ||c\mathbf{x}_i||_1 \,.$$

Thus, the norm of $c\mathbf{x}_i$ increases under the action of M_A for small positive c. The same is true for each i. If we let $c^* = \min_{i=1,\ldots,k} c_i^*$ then the norm of $c\mathbf{x}_i$ increases under the action of M_A for all i if $0 < c < c^*$. Now consider any point, $\mathbf{z}$, in T_A such that $||\mathbf{z}||_1 = c$ with $0 < c < c^*$. The set of points, $T_{A,c}$, in T_A whose L^1 norm is c clearly lie on a hyperplane. The points $c\mathbf{x}_i$ lie in this hyperplane and we know that their norm is increased under M_A. Thus, using Proposition 2 the image under M_A of $T_{A,c}$ lies in a hyperplane further from the origin. That is, every point in the image has norm $> c$. An exactly parallel argument can be made for the extremals of T_B under the action of M_B, so there is a positive constant d^* such that for any point $\mathbf{z} \in T_B$ for which $0 < ||\mathbf{z}||_1 < d^*$ we have $||M_B\mathbf{z}||_1 > ||\mathbf{z}||_1$. Clearly no convergence to the origin is possible for any trajectory in T, since whenever the norm of a point on the trajectory goes below $\min\{c^*, d^*\}$ it must increase on the next iteration. ■

Again, extension to more than two cycles is straightforward.

Then, finally, as a corollary to Propositions 9 and 10 we have the following:

Corollary 11 *Under the conditions of Propositions 9 and 10, if for every* $W \in (A^*B^*)^*$*, one of the following holds:*

(a) $W(K - \{\mathbf{0}\}) \subseteq int(K)$*,*

(b) $\rho(W)$ *is simple, or*

(c) no eigenvector corresponding to $\rho(W)$ *lies in* T*,*

then the network has an attractor passing through T*, on which the dynamics must be aperiodic.*

5 Examples

The results of the previous section allow us to tackle the problem of proving existence of stable aperiodic dynamics in a network by finding a trapping region on an orthant

boundary (Poincaré section) involving two or more cycles, showing that trajectories in this region do not converge to the origin, and showing that the matrices for these cycles have a common invariant proper cone that does not intersect the trapping region (though they may share a common boundary, if we can be sure that the dominant eigenvector never lies on this shared boundary). How to find a common invariant proper cone even for a pair of matrices is a non-trivial problem that does not seem to have been addressed in the linear algebra literature. Some results for this question have been obtained at least under some conditions (particularly in $\mathbf{R}^3$) and will appear in a future publication. Here, we will simply demonstrate the existence of common invariant cones in a few examples in $\mathbf{R}^3$, but these should make the essential ideas of the method clear.

The basic idea (for matrices in $\mathbf{R}^3$, at least) is to look at intersections of invariant linear subspaces spanned by subsets of eigenvectors for each matrix, or in some cases intersections with the images of these subspaces under the action of the other matrix. For a matrix with positive real distinct eigenvalues, the cone generated by its eigenvectors, for example $\{\mathbf{u}, \mathbf{v}, \mathbf{w}\}^G$ in $\mathbf{R}^3$, is clearly invariant, no matter which of the 2^n choices of signs of the eigenvectors one picks. Such cones form a partition of $\mathbf{R}^n$ similar to that of the 2^n standard orthants of $\mathbf{R}^n$. If one of the non-dominant eigenvalues is negative, then we need to put both positive and negative multiples of its eigenvector in the cone's generating set to make it invariant. This cone then comprises two of the original 2^n cones. It is also no longer a proper cone, since it is not pointed (*i.e.*, $K \cup (-K) \neq \{\mathbf{0}\}$), so we will not be able to use the whole of it as a common invariant cone. If other eigenvalues are negative, they too will have a pair of eigenvectors of opposite sign in the generating set. If a common invariant proper cone exists for a pair of matrices, the easiest kind of candidate to check is the intersection of cones generated by the eigenvectors of each matrix. The extremals (*i.e.*, the generating set) for this cone of intersection, will in general be the intersections

of invariant subspaces of the two matrices. Our first example, below, is of this type. Such an intersection cone will not always be invariant for both matrices, however, and other candidates may have to be found, using images of invariant subspaces of one matrix under multiplication by the other matrix, or images of other extremals found by intersection. Our second example is a relatively simple one of this type. Our third example, an additive neural network, is more complicated and requires finding a common invariant proper cone for seven matrices simultaneously. This task is made somewhat easier by the fact that the matrices fall into groups with very similar eigenvalues.

5.1 Example 1

The 4-net considered by Mestl et al. [20] is given by the following set of differential equations

$$\begin{aligned} \dot{y}_1 &= -y_1 + 2(\tilde{y}_2\bar{\tilde{y}}_3 + \bar{\tilde{y}}_2\tilde{y}_3) - 1.2546 \\ \dot{y}_2 &= -y_2 + 2(\bar{\tilde{y}}_1\bar{\tilde{y}}_4 + \tilde{y}_1\tilde{y}_4) - 1.3762 \\ \dot{y}_3 &= -y_3 + 2\tilde{y}_1\tilde{y}_2 - 0.8024 \\ \dot{y}_4 &= -y_4 + 2(\bar{\tilde{y}}_1\bar{\tilde{y}}_3 + \tilde{y}_3) - 1.2682 \end{aligned} \tag{12}$$

where $\bar{\tilde{y}}_i = 1 - \tilde{y}_i$ and $\tilde{y}_i$ is as defined in Equation 2.

The focal point coordinates, $F_i(\tilde{\mathbf{y}})$, for a given orthant $\tilde{\mathbf{y}}$ may be calculated from the equations. For example, when $\mathbf{y}$ is in the positive orthant, we have $\tilde{\mathbf{y}} = (1, 1, 1, 1)$ and $\mathbf{F} = (-1.2546, 0.6238, 1.1976, 0.7318)$.

The logical structure of the network, *i.e.*, the directions of flow across orthant boundaries, can be depicted as a directed graph on a four-dimensional hypercube, or 4-cube (Figure 1). The vertices represent orthants of phase space and the directed edges represent the direction of flow across the boundary between a pair of orthants. The vertex labels correspond to the value of $\tilde{\mathbf{y}}$ in each orthant (essentially the sign

structure of the orthant).

Starting on the edge between 0011 and 1011, we encounter the following vertices in defining two cycles:

$$A : 1011 \to \mathbf{1111} \to 1101 \to 1100 \to 1000 \to 0000 \to 0010 \to 0110 \to 0111 \to 0011,$$

$$B : 1011 \to \mathbf{1001} \to 1101 \to 1100 \to 1000 \to 0000 \to 0010 \to 0110 \to 0111 \to 0011.$$

The labels A and B can be taken to be the matrices in the two mappings corresponding to these two cycles. Letting $\mathbf{x} = (x_1, x_2, x_3)' = (y_2, y_3, y_4)'$, the mappings are

$$M_A\mathbf{x} = \frac{A\mathbf{x}}{1 + \langle \phi, \mathbf{x} \rangle}, \qquad M_B\mathbf{x} = \frac{B\mathbf{x}}{1 + \langle \psi, \mathbf{x} \rangle}, \tag{13}$$

where

$$\begin{aligned} A &= \begin{pmatrix} -10.613261 & -9.804502 & -3.452968 \\ 2.105432 & 4.747100 & 2.991261 \\ 6.394689 & 5.771168 & 1.934729 \end{pmatrix}, \\ \phi &= (4.919877, 11.494663, 6.269858)', \end{aligned}$$

$$\begin{aligned} B &= \begin{pmatrix} 0.400545 & -1.242174 & -3.452968 \\ 4.743815 & 6.798225 & 2.991261 \\ -0.264146 & 0.594472 & 1.934729 \end{pmatrix}, \\ \psi &= (9.789031, 15.280029, 6.269858)'. \end{aligned}$$

The details of how these mappings are calculated can be found in References [20] or [16] but note that there is a typographical error in Equation (4.3) in Reference [20]. Since we start on the boundary between the 0011 and 1011 orthants, the maps apply to the boundary $(0, -, +, +)$ in $\mathbf{R}^4$ or the $(-, +, +)$ octant of $\mathbf{R}^3$ and are only defined on a cone in this octant, their respective returning cones. The eigenvalues and corresponding eigenvectors of matrix A are

$$\lambda_1 = -8.291439, \qquad \lambda_2 = 4.387496, \qquad \lambda_3 = -0.027489,$$

$$\mathbf{u}_A = \begin{pmatrix} -11.134116 \\ 0.230442 \\ 6.832402 \end{pmatrix}, \quad \mathbf{v}_A = \begin{pmatrix} -0.244180 \\ 0.326903 \\ 0.132569 \end{pmatrix}, \quad \mathbf{w}_A = \begin{pmatrix} 0.443301 \\ -0.842145 \\ 1.032191 \end{pmatrix},$$

and similarly for matrix B

$$\mu_1 = 5.652616\,, \qquad \mu_2 = 3.429296\,, \qquad \mu_3 = 0.051588\,,$$

$$\mathbf{u}_B = \begin{pmatrix} -0.128914 \\ 0.359718 \\ 0.066676 \end{pmatrix}, \quad \mathbf{v}_B = \begin{pmatrix} -0.313318 \\ 0.289705 \\ 0.170607 \end{pmatrix}, \quad \mathbf{w}_B = \begin{pmatrix} 0.812294 \\ -0.722844 \\ 0.342127 \end{pmatrix},$$

When the eigenvalues are distinct we use the convention that $\mathbf{u}$, $\mathbf{v}$ and $\mathbf{w}$ correspond to the eigenvalues in order of decreasing modulus, and likewise the indices of the eigenvalues in the order $1, 2, 3$. The eigenvectors above are in fact fixed points of the respective maps M_A and M_B, the unique ones on each eigenvector, from Equation 9. Note that only $\mathbf{u}_A$, $\mathbf{v}_A$, $\mathbf{u}_B$ and $\mathbf{v}_B$ are in the orthant boundary to which the map applies.

Using Equations 7 and 8 the returning cone, C_A, for the A matrix is defined by

$$R_A = \begin{pmatrix} -8.886421 & -4.717095 & -0.016935 \\ 2.264171 & 1.680946 & 0.297248 \\ 1.603078 & 1.246261 & 0.000000 \end{pmatrix},$$

and C_B is defined by

$$R_B = \begin{pmatrix} 6.346434 & 7.125196 & -0.016935 \\ -0.154213 & -0.199149 & 0.297248 \\ -1.603078 & -1.246261 & 0.000000 \end{pmatrix}.$$

Thus, for example, $\mathbf{x} \in C_A$ if $R_A\mathbf{x} \geq \mathbf{0}$ (i.e., is nonnegative).

A calculation now shows that $\mathbf{u}_A \notin C_A$ and $\mathbf{u}_B \notin C_B$, but $\mathbf{v}_A \in C_A$ and $\mathbf{v}_B \in C_B$. Therefore, $\mathbf{v}_B$ is an unstable fixed point of the B cycle, since it corresponds to an eigenvalue of B that is not the dominant one (Proposition 5). Similarly, $\mathbf{v}_A$ is an unstable fixed point of the A cycle.

This network has a trapping region in the $(0, -, +, +)$ boundary [20], shown schematically in Figure 2. The point $\mathbf{v}_B$, called F_{B3} in Reference [20], (note that the labels F_{B1} and F_{B3} are transposed in Table 2 in Reference [20][1]), and $\mathbf{v}_A$, called

[1]Small discrepancies in some of the numbers given here and in Reference [20] are most likely due to their reporting only four decimal places in the constants in their differential equations, when they may have actually used more in some of their calculations. We stick here to the values exactly as written in their equations.

F_{A3} in Reference [20], are shown in the figure. The stable and unstable manifolds of these points are indicated by the arrows. In the figure, everything is projected onto a plane orthogonal to the vector $\mathbf{v}_A$, so the planar regions really represent cross sections of cones and points in the figure represent rays emanating from the origin. Some license has been taken in distorting the figure to make the regions clearer — the shaded region is actually very thin. It can be shown that the fractional linear maps associated with trajectories in these networks take straight lines to straight lines (Proposition 2), and this applies also to projections onto a plane [16]. The line through S_1 and S_2 is the separating boundary between the domains of definition (i.e., returning cones) of the A and B cycles (actually a plane projected onto a line in the figure). The dot-dash lines in Figure 2 indicate the domains of definition of these two cycles. The large letters show which cycle applies in which region. S_1 is the intersection of the stable manifold, W_B^s, of $\mathbf{v}_B$ and the separating boundary (again projected onto the plane). S_2 is the intersection of the unstable manifold, W_B^u, of $\mathbf{v}_B$ and the separating boundary. S_3 is the intersection of W_B^u and the inverse image under M_A of W_B^s. Let T_A be the triangular region (the projection of a triangular cone) with vertices S_1, S_2 and S_3, let T_B be the triangular region with vertices $\mathbf{v}_B$, S_1 and S_2, and let $T = T_A \cup T_B$. Then T is mapped into the shaded regions. Note that by their definitions, $M_B\mathbf{v}_B = \mathbf{v}_B$, M_BS_1 and M_AS_3 lie on W_B^s, and M_BS_2 lies on W_B^u. Also, it can be checked that M_A and M_B coincide on the boundary between their domains. Thus, T is invariant under the network dynamics.

This establishes the existence of the trapping region, as described by Mestl *et al.* [20]. We now show that the matrices A and B have a common invariant proper cone. Again, we use a projection in order to visualize the regions under consideration, but for this purpose we find it more convenient to project onto the unit sphere because more than one octant will typically be involved. Thus, polyhedral cones in $\mathbf{R}^3$ become polygonal regions on the surface of the unit sphere.

Recall the notation for a cone as generated by a set of vectors, so that for example

$$\{\mathbf{u}, \mathbf{v}\}^G = \{\mathbf{x} | \mathbf{x} = c_1\mathbf{u} + c_2\mathbf{v} \text{ for some } c_1 \geq 0, c_2 \geq 0\}.$$

Let

$$\begin{aligned} \mathbf{z}_1 &= \{-\mathbf{u}_B, \mathbf{w}_B\}^G \cap \{\mathbf{u}_A, -\mathbf{v}_A\}^G, \\ \mathbf{z}_2 &= \{\mathbf{v}_B, \mathbf{w}_B\}^G \cap \{\mathbf{u}_A, \mathbf{v}_A\}^G. \end{aligned}$$

Then we claim that the cone generated by $\mathbf{v}_B$, $-\mathbf{u}_B$, $\mathbf{z}_1$ and $\mathbf{z}_2$, *i.e.*,

$$K = \{\mathbf{v}_B, -\mathbf{u}_B, \mathbf{z}_1, \mathbf{z}_2\}^G,$$

is invariant for both $-A$ and B (see Figure 3). Since matrix multiplication is linear, to show that the cone K is invariant, we need only check that its extremal vertices are mapped back into the cone under each matrix multiplication. Clearly, $B\mathbf{v}_B = \mu_2\mathbf{v}_B$ so the ray through $\mathbf{v}_B$ is mapped to itself under multiplication by B. Similarly, $B(-\mathbf{u}_B) = -\mu_1\mathbf{u}_B$. Since $\{\mathbf{v}_B, \mathbf{w}_B\}^G \in W_B^s$ and $\mu_2 > 0$, we have $B\mathbf{z}_2 \in \{\mathbf{v}_B, \mathbf{z}_2\}^G$. Similarly, since $\{-\mathbf{u}_B, \mathbf{w}_B\}^G$ is part of the stable invariant manifold of $-\mathbf{u}_B$ and $\mu_1 > 0$, we have $B\mathbf{z}_1 \in \{-\mathbf{u}_B, \mathbf{z}_1\}^G$. Thus, $BK \subseteq K$.

Now, multiplying by $-A$, it is clear that $-A\mathbf{z}_1 \in \text{span}(\mathbf{u}_A, \mathbf{v}_A)$ and a calculation shows that in fact $-A\mathbf{z}_1 \in \{\mathbf{u}_A, \mathbf{z}_2\}^G$ (note that $-A$ has eigenvalue $-\lambda_2 < 0$ so there is reflection about $\{\mathbf{u}_A, \mathbf{w}_A\}^G$). Similarly, $-A\mathbf{z}_2 \in \text{span}(\mathbf{u}_A, \mathbf{v}_A)$ and a calculation shows that $-A\mathbf{z}_2 \in \{\mathbf{u}_A, \mathbf{z}_1\}^G$. Since multiplication by $-A$ contracts towards $\text{span}(\mathbf{u}_A, \mathbf{v}_A)$, it is clear that the points $\mathbf{v}_B$ and $-\mathbf{u}_B$ will be taken closer to $\text{span}(\mathbf{u}_A, \mathbf{v}_A)$. A calculation is needed again, however, to verify that they are taken inside the narrow sides of the cone. This then implies that $-AK \subseteq K$, and therefore $AK \subseteq (-K)$. These points are shown in Figure 3.

Furthermore, while B takes every extremal point of K to the boundary of K and A takes two of the extremal points to the boundary of K, it is not difficult to see

that if a cycle involves both A and B, all extremal points will be taken to int(K). The points $A\mathbf{z}_1$ and $A\mathbf{z}_2$ are taken by B to the interior of K and $\mathbf{v}_B$ and $-\mathbf{u}_B$ are already taken to int(K) by A. We have already checked that A and B themselves do not have a dominant eigenvector in T_A or T_B respectively, and thus do not correspond to stable periodic orbits, so that only leaves us to check combinations, W, involving both A and B. These satisfy the condition $W(K - \{\mathbf{0}\}) \subseteq \text{int}(K)$.

In order to apply Proposition 9, we need to show that $(K \cup (-K)) \cap T = \{\mathbf{0}\}$. This is not quite true here, since $K \cap T = \{\mathbf{v}_B, \mathbf{z}_2\}^G$. However, there is actually a smaller trapping region within T that does not include this boundary [23]. Also, any point on this boundary is mapped under $-A$ to the interior of the invariant cone, and no point from the interior of the cone can be mapped back to this boundary under either $-A$ or B. Therefore, points on this boundary could not be eigenvectors for multiple products of matrices $-A$ and B, except in the case that the product consists only of the B matrix, in which case the eigenvector on the boundary is $\mathbf{v}_B$ itself, which we already know is not dominant.

Either way, we have established that there exist a disjoint T and $K \cup (-K)$. By proposition 9, there cannot exist a stable periodic orbit through T. Thus, the dynamics on the attractor in this trapping region for the matrices acting on rays, or equivalently for the attractor's projection onto the plane of Figure 2, are aperiodic. However, we must still show that trajectories do not converge to the origin. This can be confirmed by checking that $||A\mathbf{x}_i|| > 1$ and $||B\mathbf{y}_i|| > 1$ for unit vectors $\mathbf{x}_i$ and $\mathbf{y}_i$ at the corners of the regions T_A and T_B, respectively. The unit extremal vectors can be calculated by intersections of the planes defined by rows of R_A and R_B with each other and with the boundaries of the octant. For example, $\mathbf{v}_B$ is an extremal vector of the region T_B, and

$$B\frac{\mathbf{v}_B}{||\mathbf{v}_B||_1} = 3.429435 > 1\,.$$

The other calculations are similar and show by Proposition 10 that trajectories in

T cannot converge to the origin. Finally, by Corollary 11, trajectories through T converge to an attractor on which the dynamics are aperiodic.

5.2 Example 2

Another 4-net with apparently irregular dynamics is given by the differential equations

$$\begin{aligned}
\dot{y}_1 &= -y_1 + 2(\bar{\tilde{y}}_3\tilde{y}_4 + \tilde{y}_2\tilde{y}_3) - 1 \\
\dot{y}_2 &= -y_2 + 2(\tilde{y}_1\bar{\tilde{y}}_3\tilde{y}_4 + \bar{\tilde{y}}_1\tilde{y}_3\tilde{y}_4 + \bar{\tilde{y}}_1\bar{\tilde{y}}_3\bar{\tilde{y}}_4) - 1 \\
\dot{y}_3 &= -y_3 + 2(\bar{\tilde{y}}_1\tilde{y}_2 + \tilde{y}_1\tilde{y}_4) - 1 \\
\dot{y}_4 &= -y_4 + 2(\tilde{y}_2\bar{\tilde{y}}_3 + \bar{\tilde{y}}_1\tilde{y}_3) - 1
\end{aligned} \tag{14}$$

where again $\bar{\tilde{y}}_i = 1 - \tilde{y}_i$. Note that for this network the focal point coordinates are all ± 1. If we consider a Poincaré section on the boundary $(+,+,+,0)$, there are two cycles of interest, which we again call A and B:

$A : 1110 \to 1010 \to 0010 \to 0000 \to 0100 \to \mathbf{0110} \to 0111 \to 1111,$

$B : 1110 \to 1010 \to 0010 \to \mathbf{0011} \to \mathbf{0001} \to 0000 \to 0100 \to \mathbf{0101} \to 0111 \to 1111,$

with Poincaré mappings defined by Equations 13, where now

$$\begin{aligned}
\mathbf{x} &= (x_1, x_2, x_3)' = (y_1, y_2, y_3)', \\
A &= \begin{pmatrix} -3 & -8 & 4 \\ -2 & -5 & 2 \\ -4 & -12 & 7 \end{pmatrix}, \\
\phi &= (-4, -14, 10)', \\
B &= \begin{pmatrix} 5 & 8 & 0 \\ 6 & 11 & -2 \\ 12 & 20 & -1 \end{pmatrix}, \\
\psi &= (12, 18, 2)'.
\end{aligned}$$

The eigenvalues of A are $\lambda_1 = -4.627213$, $\lambda_2 = 3.685846$ and $\lambda_3 = -0.058633$. The eigenvalues of B are $\mu_1 = 12.532871$, $\mu_2 = 2.434352$ and $\mu_3 = 0.032777$. The

returning cones, C_A and C_B, for the A and B matrices respectively are determined by

$$R_A = \begin{pmatrix} -2 & -5 & 2 \\ 2 & 4 & -1 \end{pmatrix}, \quad R_B = \begin{pmatrix} 6 & 11 & -2 \\ -2 & -4 & 1 \end{pmatrix}.$$

These define cones:

$$C_A = \left\{ \left(0, \frac{2}{7}, \frac{5}{7}\right)', \left(\frac{1}{2}, 0, \frac{1}{2}\right)', \left(\frac{1}{3}, 0, \frac{2}{3}\right)', \left(0, \frac{1}{5}, \frac{4}{5}\right)' \right\}^G, \tag{15}$$

$$C_B = \left\{ \left(0, \frac{2}{13}, \frac{11}{13}\right)', \left(\frac{1}{4}, 0, \frac{3}{4}\right)', \left(\frac{1}{3}, 0, \frac{2}{3}\right)', \left(0, \frac{1}{5}, \frac{4}{5}\right)' \right\}^G, \tag{16}$$

on which the Poincaré maps are defined for each cycle. We take $T_A = C_A$ and $T_B = C_B$. A has only its second eigenvector, $\mathbf{v}_A$ (corresponding to the eigenvalue with second largest modulus), in its returning cone, T_A. B has none in T_B. It turns out that $T = T_A \cup T_B$ is a trapping region for the network. This can be established simply by verifying that $M_A(T_A) \subseteq T$ and $M_B T_B \subseteq T$. The regions T_A and T_B as well as their images are depicted in Figure 4.

Once again, we use cones defined by eigenvectors of the A and B matrices and their images, to construct a common invariant proper cone, K (Figure 5). Again, we use $-A$, since $\lambda_1 < 0$. We define

$$\begin{aligned} \mathbf{z}_1 &= \{\mathbf{u}_B, \mathbf{v}_B\}^G \cap \{\mathbf{u}_A, \mathbf{w}_A\}^G), \\ \mathbf{z}_2 &= \{\mathbf{u}_B, \mathbf{w}_B\}^G \cap \{\mathbf{u}_A, \mathbf{v}_A\}^G. \end{aligned}$$

Then we claim that

$$K = \{\mathbf{u}_B, \mathbf{z}_2, -A\mathbf{z}_2, \mathbf{z}_1\}^G$$

is an invariant cone for both A and B. Clearly, $B\mathbf{u}_B = \mu_1 \mathbf{u}_B$, $B\mathbf{z}_1 \in \{\mathbf{u}_B, \mathbf{z}_1\}^G$ and $B\mathbf{z}_2 \in \{\mathbf{u}_B, \mathbf{z}_2\}^G$. A calculation shows that $B(-A\mathbf{z}_2) \in \text{int}(K)$. Also, $-A\mathbf{z}_1 \in \text{int}\{\mathbf{u}_A, \mathbf{z}_1\}^G \subseteq \text{int}(K)$, since $-\lambda_1 > 0$ and $-\lambda_3 > 0$. By definition, $-A\mathbf{z}_2 \in K$. While $-A(-A\mathbf{z}_2) \in \text{span}(\mathbf{z}_2, -A\mathbf{z}_2)$, a calculation is needed to confirm that $-A(-A\mathbf{z}_2) \in \{\mathbf{z}_2, \mathbf{u}_A\}^G$. Finally, another calculation shows that $-A\mathbf{u}_B \in \text{int}(K)$. See Figure 5.

Again, although A and B individually map some extremal points to the boundary of K, calculation of $-AB\mathbf{z}_1$, $-AB\mathbf{z}_2$ as well as $-A\mathbf{u}_B$ mentioned above shows that all are in int(K), as is $B(-A\mathbf{z}_2)$ so any cycle involving both A and B maps K to int(K). We have already noted that A and B individually do not have dominant eigenvectors in T.

Thus, $K \cup (-K)$ is invariant for both A and B, and is disjoint from T. Proposition 9 then guarantees that there are no stable periodic orbits through the trapping region T. We omit the straightforward calculations showing that $||A\mathbf{x}_i||_1 > 1$ for each unit extremal of T_A, as listed in Equation 15, and similarly for extremals of T_B, as listed in Equation 16. Then Corollary 11 may be applied to conclude that the network must have stable aperiodic dynamics in T.

5.3 Example 3

We now deal with an example that fits into the framework of additive neural networks, *i.e.*, Equations 1 and 2 with F_i given by Equation 3. The analysis in this example turns out to be more complicated but the method is the same and it illustrates how the method can sometimes be extended to situations where more than two cycles are involved.

The network is defined by Equations 1, 2 and 3, *i.e.*

$$\dot{\mathbf{y}} = -\mathbf{y} + W\tilde{\mathbf{y}} - \tau \tag{17}$$

with

$$W = \begin{pmatrix} 0 & 10 & 6 & -2 \\ -4 & 0 & 1 & -5 \\ -8 & -8 & 0 & 3 \\ 1 & -2 & -9 & 0 \end{pmatrix},$$

$$\tau = (0.5, -3.5, -0.5, -0.5)'.$$

Note that there is still no self-input in the network. The dynamics of this network can be captured by looking at cycles starting at and returning to the boundary between

orthants 1100 and 1000, *i.e.*, the boundary $(+, 0, -, -)$. Five cycles are possible on this boundary:

$$A: 1000 \to 1001 \to 0001 \to 0011 \to 0010 \to 1010 \to 1000 \to 0000 \to 0100 \to 1100,$$

$$B: 1000 \to 0000 \to 0100 \to 1100,$$

$$C: 1000 \to 1001 \to 0001 \to 0011 \to 0010 \to 0110 \to 1110 \to 1100,$$

$$D: 1000 \to 0000 \to 0001 \to 0011 \to 0010 \to 0110 \to 1110 \to 1100,$$

$$E: 1000 \to 1001 \to 0001 \to 0011 \to 0010 \to 1010 \to 1110 \to 1100.$$

The mappings and returning cones for each cycle can be calculated as before (again for details, see Reference [16]). They are depicted in Figure 6. Let the mappings (Equation 6) for each cycle be called M_i, $i = A, B, C, D, E$, and the matrices in the mappings we denote A, B, C, D and E. Without giving all the details, we outline the procedure for identifying a trapping region and finding a common invariant proper cone. The entire octant $(+, -, -)$ is a trapping region, as it is the union of returning cones of the five cycle maps, and each cycle mapping M_A to M_E maps its returning cone back into this octant. The images of the five returning cones under their respective mappings are also shown in Figure 6. Starting in this octant, after one mapping we must fall somewhere in the union of the images of the five regions, so this union is also a trapping region.

When we look for a common invariant proper cone, we find that we cannot work with the matrix A in cycle map M_A since its dominant eigenvalues are complex and these produce rotations in a plane through the origin that preclude any invariant cone being proper ($K \cap (-K) \neq \{\mathbf{0}\}$). In fact it is an obvious consequence of Theorem 6 that if $\rho(A)$ is not an eigenvalue, A can leave no proper cone invariant. Thus we need to look at combinations in which cycle A can occur. We define a trapping region

$$T^* = M_B(C_B) \cup M_C(C_C) \cup M_D(C_D) \cup M_E(C_E) \cup (M_A(C_A) \cap C_B)$$

where C_i is the returning cone for cycle mapping M_i. To confirm that this is a trapping region, we need to verify that those parts of T^* lying in C_A are indeed mapped back into T^*, *i.e.*, are mapped into $M_A(C_A) \cap C_B$. It is a matter of calculation to show that $M_A(M_C(C_C) \cap C_A) \in M_A(C_A) \cap C_B$, and likewise for $M_A(M_D(C_D) \cap C_A)$ and $M_A(M_B(C_B) \cap C_A)$. $M_E(C_E)$ does not intersect C_A. Now we observe that once in the trapping region, if we go through cycle A, it must be followed by cycle B, and it must be preceded either by cycle B, C or D. If it is preceded by cycle B, that is if we land in $M_B(C_B) \cap C_A$, then it turns out that the only part of C_B within the trapping region we could have come from is that part in $M_C(C_C)$, which can be verified by calculating the inverse image under M_B of $M_B(C_B) \cap C_A$. Thus, if we go through cycles B and A in succession, then the cycle before must have been C and the cycle after must be B again. In summary, the only combinations in which cycle A can occur are (C, A, B), (D, A, B), and (C, B, A, B). We will call these cycles F, G and H, so that $M_F = M_B \circ M_A \circ M_C$, for example. The matrices in these mappings will be called

$$\begin{aligned} F &= BAC\,, \\ G &= BAD\,, \\ H &= BABC\,. \end{aligned}$$

All trajectories through the trapping region, T^*, consist of compositions of the seven cycles B through H. Thus, the task is now to find a common invariant proper cone for the seven matrices B through H. As C, D and E have a negative dominant eigenvalue, we will actually use $-C$, $-D$ and $-E$. An appropriate invariant cone is shown projected onto the unit sphere in Figure 7. The cone is

$$K = \{\mathbf{k}_1, \mathbf{k}_0, CC\mathbf{k}_0, \mathbf{k}_2, \mathbf{k}_3, -C\mathbf{k}_0, \mathbf{k}_4\}^G\,,$$

where

$$\mathbf{k}_0 \;=\; \mathbf{u}_{HC}\,,\ \text{the dominant eigenvector of matrix } HC\,,$$

$$
\begin{aligned}
\mathbf{k}_1 &= \{\mathbf{u}_H, \mathbf{w}_H\}^G \cap \{x_1 = 0\}\,, \\
\mathbf{k}_2 &= \{CC\mathbf{k}_0, EC\mathbf{k}_0\}^G \cap \{\mathbf{u}_E, \mathbf{v}_E\}^G\,, \\
\mathbf{k}_3 &= \{-C\mathbf{k}_0, -E\mathbf{k}_0\}^G \cap \{\mathbf{u}_E, -\mathbf{v}_E\}^G\,, \\
\mathbf{k}_4 &= \{\mathbf{u}_E, \mathbf{w}_E\}^G \cap \{x_1 = 0\}\,.
\end{aligned}
$$

In the figure, the generating points of the cones are marked by circles. The point $\mathbf{k}_1$ is at the intersection of the line from $\mathbf{w}_H$ to $\mathbf{u}_H$ and the line marked W_B, which is the eigenspace for the matrix B, for which all three eigenvalues are 1. The rest are, counterclockwise from $\mathbf{k}_1$: $\mathbf{k}_0$, $CC\mathbf{k}_0$, $\mathbf{k}_2$, $\mathbf{k}_3$, $-C\mathbf{k}_0$, $\mathbf{k}_4$. It is clear that matrix $-C$ maps $\mathbf{k}_0$ to $-C\mathbf{k}_0$ and $-C\mathbf{k}_0$ to $CC\mathbf{k}_0$. Also, $-E$ maps $\mathbf{k}_0$ to the boundary between $-C\mathbf{k}_0$ and $\mathbf{k}_3$ and $-C\mathbf{k}_0$ to the boundary between $CC\mathbf{k}_0$ and $\mathbf{k}_2$. Furthermore $\mathbf{k}_2$ and $\mathbf{k}_3$ lie on a stable manifold of the dominant eigenvector of $-E$, namely $\mathbf{u}_E$, and $-E\mathbf{k}_2$ and $-E\mathbf{k}_3$ lie on the boundary of the invariant cone between $\mathbf{k}_2$ and $\mathbf{k}_3$. B maps $\mathbf{k}_1$ and $\mathbf{k}_4$ to themselves and H maps $\mathbf{k}_0$ to itself. Every other mapping of extremal vector for K by one of the seven matrices lands in the interior of K, as can be confirmed by direct calculation.

Careful inspection of the cases where an extremal point of K is mapped to the boundary of K shows that there are nevertheless few words W composed of our seven matrices that still map any point of K to its boundary. Clearly, B, $-C$, $-E$ and H do so, as discussed above. Figure 6 shows that $M_E(C_E) \in C_B$ entirely, so E can only be followed by B. B maps every point left on the boundary by $-E$ to $\mathrm{int}(K)$, *i.e.*, $-BE(K - \{\mathbf{0}\}) \subseteq \mathrm{int}(K)$. B maps $\mathbf{k}_1$ and $\mathbf{k}_4$ to themselves, but any other matrix maps these points to $\mathrm{int}(K)$. Although $-C$ maps $-C\mathbf{k}_0$ to $CC\mathbf{k}_0$, another extremal point, any subsequent multiplication takes this point to $\mathrm{int}(K)$. Finally, $\mathbf{k}_0$ is mapped by $-C$ to $-C\mathbf{k}_0$, an extremal point, and $-C\mathbf{k}_0$ is mapped by H back to $\mathbf{k}_0$, by the definition of that point as an eigenvector of HC. Thus, aside from the four individual matrices above, the one other possible cycle that does not map K to

int(K) is $H(-C)$. Checking the eigenvectors of the matrices $-C$, $-E$, H and $-HC$ shows that only $-C$ has an eigenvector in its returning cone, and it is the second, not the dominant eigenvector. B, however, has a two-dimensional eigenspace associated with its one eigenvalue ($\mu = 1$), and has to be treated carefully. In principal, a matrix with dominant eigenvalue 1 can have invariant sets on which trajectories spiral in to the origin (or another fixed point on a coordinate subspace).

The matrix

$$B = \begin{pmatrix} 1 & 0 & 0 \\ -\alpha & 1 & 0 \\ \beta & 0 & 1 \end{pmatrix},$$

where $\alpha = \frac{2208}{133}$ and $\beta = \frac{408}{133}$, is lower triangular with all eigenvalues 1. Its eigenspace is the subspace $\{x_1 = 0\}$. Thus, although the Krein-Rutman theorem guarantees that an eigenvector for eigenvalue $\rho(B) = 1$ lies in K, it need not be unique (up to scalar multiples). In fact, here the entire two-dimensional eigenspace consists of eigenvectors corresponding to eigenvalue 1, and in particular, one boundary of the trapping region. If we start on this boundary of the trapping region where $x_1 = 0$, we stay on it, and thus continue to iterate the cycle mapping M_B, which will drive us in to the origin. However, there is no requirement that the trapping region be closed. We will therefore show that

$$T = T^* \cap \{x_1 > 0\}$$

is also a trapping region. No matrix other than B maps any point of T to $\{x_1 = 0\}$. Thus, we need only confirm that if we start away from $\{x_1 = 0\}$ in T, then in a finite number of iterations we leave B's returning cone, C_B, thus preventing convergence to $\{x_1 = 0\}$. Points in the interior of region C_B in Figure 6 are mapped upwards, as well as closer to the boundary where $x_1 (= y_1) = 0$. To show that they must eventually cross the upper boundary of C_B, we first calculate that this boundary has slope $-22/7$. If we let $\mathbf{a} = (a, -b, -c)'$, with $a, b, c \geq 0$, so that the ratio of the x_3 to

x_1 components is $-c/a$, then

$$B\mathbf{a} = (a, -b - \alpha a, -c + \beta a)'$$

and the ratio of the x_3 to x_1 component is $-c/a + \beta$. Thus, each multiplication by B increases this ratio by more than 3. Any point in C_B away from $\{x_1 = 0\}$ has some fixed finite ratio of third to first components. Thus, only a finite number of multiplications by B are required to increase this ratio above $-22/7$ (but still below 0, since $\beta < 22/7$). The trajectory of any such point thus starts with a finite sequence of B's before continuing with some other of our cycles, and it is not possible to converge to $\{x_1 = 0\}$. Thus, T is truly a trapping region, and B itself does not correspond to a periodic orbit through T or a stable spiral fixed point in T.

While the invariant cone, K, does encroach on the $(+, -, -)$ octant, the region of that octant that it includes is disjoint from the trapping region depicted in Figure 6. In fact, $T \cap (K \cup (-K)) = \{\mathbf{0}\}$. With the exceptions that have already been eliminated, any word, W made up of the seven cycle matrices, maps $K - \{\mathbf{0}\}$ into its interior, so that Proposition 9 implies that no stable periodic orbit passes through T.

Finally, we need to apply Proposition 10, extended in a natural way to more than two mappings and regions, to show that there is no convergence to the origin. It is easiest to apply this to the five cycle matrices A through E (rather than working with the composite mappings F, G and H, and to check the extremals of the returning cones C_A through C_E rather than working with the smaller trapping region we used above. If convergence to the origin is impossible in the entire orthant boundary (*i.e.*, $\mathcal{O}^{(0)} = C_A \cup C_B \cup C_C \cup C_D \cup C_E$) then it is certainly impossible in the trapping region, $T \subseteq \mathcal{O}^{(0)}$. However, the norms of the matrices multiplied by respective unit extremals are in this case not all > 1. The two exceptions are $||B\mathbf{u}_B||_1 = 1$ and $||B\mathbf{v}_B||_1 = 1$, where $\mathbf{u}_B = (0, -1, 0)'$ and $\mathbf{v}_B = (0, 0, -1)'$. We know of course that convergence to the origin is possible on the plane $x_1 = 1$, but we showed above that trajectories cannot converge to this plane from inside T. A similar argument can be made here to

extend Proposition 10 to cover this case. Note first that $B\mathbf{u}_B = \mathbf{u_B}$ and $B\mathbf{v}_B = \mathbf{v_B}$. While B may occur several times in succession, it was shown above that it must eventually be followed by one of the other cycle matrices along a trajectory starting in T. Clearly, $||AB^m\mathbf{u}_B||_1 = ||A\mathbf{u}_B||_1$ and similarly for the other matrices and for $\mathbf{v}_B$. So, if these values are all > 1, we still cannot have convergence along trajectories from points in T. This is confirmed by calculations which we omit. Again, Corollary 11 is then invoked to conclude that there is an attractor in T on which the dynamics are aperiodic.

6 Discussion

We have presented a general method by which the existence of an attractor on which the dynamics is aperiodic may be proven analytically for a given Glass network. The class of Glass networks is quite broad, the functional form of the right-hand-sides of the equations being almost completely arbitrary, as long as the interactions between network units depend only on the output of the response function of other units. The form of the response is a step function but the indications are that the same behaviour will be found in networks where the response function is a steep sigmoid. Thus, the functional forms of many neural network models are encompassed in this class, including additive networks as well as those involving quadratic or higher order product terms. However, the results of this method will be less applicable to these networks with shallower sigmoids. Numerical work shows that in general as the slope of the sigmoid is decreased the complexity of the dynamics decreases [4, 5].

Within the class of Glass networks the method is quite general and the results we established above are valid for networks in any number of dimensions, n. However, in practice it may not be possible to apply the method, particularly for large n. Even when $n = 4$, there are examples for which the method has not so far proven successful, such as the example presented in References [21, 16], due to the difficulty of finding

(or perhaps the non-existence of) a common invariant proper cone for a large number of matrices.

The method of proof presented here depends on being able to find a non-trivial (fully n-dimensional) trapping region to begin with, and then being able to find a common invariant proper cone for all the cycle matrices of cycle maps defined on some part of the trapping region. The trick is to find a trapping region and common proper invariant cone that do not intersect. While this can sometimes be difficult, our Example 3 shows that there is some room for refinement in the method. While general results for these problems do not seem to exist in the matrix theory literature yet, good candidates for appropriate common invariant cones are ones constructed out of intersections of invariant subspaces through eigenvectors and the images of these subspaces under the matrices involved.

Also, our approach only guarantees stable aperiodic behaviour. It does not distinguish between different types of aperiodic behaviour, such as quasi-periodic and chaotic. Quasi-periodicity is very special and it seems certain that it is not present in the examples explored here, but further investigation into this distinction would be of interest.

While our method clearly has limitations, it would seem to be the first *general* approach to the analytic proof of *stable* complex behaviour in neural or other networks. Previous analytic work, as discussed in Section 1, relies on special structures built from known chaotic equations or systems.

While proof of the existence of stable complex activity in systems of differential equations is clearly of great mathematical interest, the utility of complicated dynamics in neural networks, whether biological or artificial, is still debated. It may be that complicated activity of any type (chaotic, quasi-periodic or very complicated periodic) is functionally equivalent, for example, if such activity is to act as a 'not recognized' response in an attractor neural network setting. On the other hand, the ergodicity of

chaotic dynamics on an attractor may be an important distinction from other types of complicated activity, as argued for example by Skarda and Freeman [1] and by Kaneko [2]. In any case, it may well be important in applications to distinguish between transients and attractors — to know whether complicated activity is stable or is temporary and leads eventually to a stable limit cycle or fixed point. Even in applications, claims for chaos or complex dynamics based on numerical evidence is never completely satisfactory. The current work contributes to putting such claims on a rigorous foundation.

References

[1] C. A. Skarda and W. J. Freeman, How brains make chaos in order to make sense of the world, Behavioral and Brain Sciences 10 (1987) 161–195.

[2] K. Kaneko, Cooperative behaviour in networks of chaotic elements, in: The Handbook of Brain Theory and Neural Networks, M. A. Arbib, ed. (MIT Press, Cambridge, Mass., 1995) 258–261.

[3] L. Glass, Chaos in Neural Systems, in: The Handbook of Brain Theory and Neural Networks, M. A. Arbib, ed. (MIT Press, Cambridge, Mass., 1995) 186–189.

[4] J. E. Lewis and L. Glass, Steady states, limit cycles, and chaos in models of complex biological networks, International Journal of Bifurcation and Chaos 1 (1991) 477–483.

[5] J. E. Lewis and L. Glass, Nonlinear dynamics and symbolic dynamics of neural networks, Neural Computation 4 (1992) 621–642.

[6] A. Lapedes and R. Farber, Nonlinear signal processing using neural networks: Prediction and system modelling, Technical Report LA–UR–87–2662, Los Alamos, NM: Los Alamos National Laboratory, 1987.

[7] X. Wang, Period-doublings to chaos in a simple neural network: an analytical proof, Complex Systems 5 (1991) 425–441.

[8] K. Aihara, Chaos in axons, in: The Handbook of Brain Theory and Neural Networks, M. A. Arbib, ed. (MIT Press, Cambridge, Mass., 1995) 183–185.

[9] X. Wang and E. K. Blum, Dynamics and bifurcation of neural networks, in: The Handbook of Brain Theory and Neural Networks, M. A. Arbib, ed. (MIT Press, Cambridge, Mass., 1995) 339–343.

[10] J. J. Hopfield, Neural networks and physical systems with emergent collective computational abilities, Proc. Nat. Acad. Sci. U.S.A. 79 (1982) 2554–2558.

[11] M. Cohen and S. Grossberg, Absolute stability of global pattern formation and parallel memory storage by competitive neural networks, IEEE Trans. Sys. Man Cybern. 13 (1983) 815–826.

[12] J. J. Hopfield, Neurons with graded response have collective computational properties like those of two-state neurons, Proc. Nat. Acad. Sci. U.S.A. 81 (1984) 3088–3092.

[13] A. J. Priesol, D. S. Borrett and H. C. Kwan, Dynamics of a chaotic neural network in response to a sustained stimulus, Technical Reports on Research in Biological and Computational Vision, No. RBCV-TR-91-38, Dept. of Computer Science, University of Toronto, 1991.

[14] L. Glass and J. S. Pasternack, Stable oscillations in mathematical models of biological control systems, J. Math. Biol. 6 (1978) 207–223.

[15] T. Mestl, E. Plahte and S. W. Omholt, Periodic solutions in systems of piecewise-linear differential equations, Dyn. Stab. Syst. 10 (1995) 179–193.

[16] R. Edwards, Analysis of continuous-time switching networks, Physica D 146 (2000) 165–199.

[17] L. Glass and J. S. Pasternack, Prediction of limit cycles in mathematical models of biological oscillations, Bull. Math. Biol. 40 (1978) 27–44.

[18] E. Plahte, T. Mestl and S. W. Omholt, Global analysis of steady points for systems of differential equations with sigmoid interactions, Dyn. Stab. Syst. 9 (1994) 275–291.

[19] S. A. Kauffman, Origins of Order: Self-Organization and Selection in Evolution (Oxford University Press, Oxford, 1993).

[20] T. Mestl, C. Lemay and L. Glass, Chaos in high-dimensional neural and gene networks, Physica D 98 (1996) 33–52.

[21] R. Edwards, Chaos in a continuous-time switching network, in: Proceedings of the 3rd International Conference on Dynamic Systems and Applications, Atlanta, May, 1999 (Dynamic Publishers, Atlanta, 2001) 185–192.

[22] R. Edwards and L. Glass, Combinatorial explosion in model gene networks, Chaos 10 (2000) 691–704.

[23] R. Edwards, H. Siegelmann, K. Aziza and L. Glass, Symbolic dynamics and computation in model gene networks, Chaos, (2001).

[24] T. Gedeon, Attractors in neural networks with infinte gain, preprint (2000).

[25] A. Berman and R. J. Plemmons, Nonnegative Matrices in the Mathematical Sciences (Academic Press, New York, 1994).

[26] A. Berman, M. Neumann and R. J. Stern, Nonnegative Matrices in Dynamic Systems (Wiley, New York, 1989).

Figure captions

Figure 1: The logical structure of the network from Mestl *et al.* [20]. Vertices represent orthants of phase space and edges represent the direction of flow across boundaries between orthants.

Figure 2: Sketch of the trapping region in the $(0, -, +, +)$ boundary for the network of Equation 12, projected onto a plane orthogonal to vector $\mathbf{v}_A$, the second eigenvector of matrix A in the Poincaré mapping for the A cycle. Based on Fig.4(b) in Mestl *et al.* [20]).

Figure 3: Invariant cone for the matrices A and B corresponding to Poincaré maps for the network of Equation 12, projected onto the unit sphere. Projections of the invariant subspaces through eigenvectors of A are indicated by solid lines. Projections of the invariant subspaces through eigenvectors of B are indicated by dashed lines.

Figure 4: Trapping region in the $(+, +, +, 0)$ boundary, for the network of Equation 14, projected onto a plane orthogonal to vector $(1, 1, 1)'$, with only the y_1 and y_2 components plotted. The returning cones for the A cycle and the B cycle are indicated by dotted lines and the images of these regions are indicated by solid lines. Note that the images lie withing the union of the returning cones.

Figure 5: Invariant cone for the matrices A and B corresponding to Poincaré maps for the network of Equation 14, projected onto the unit sphere, indicated by solid lines. Projections of the invariant subspaces through eigenvectors are indicated by dashed lines.

Figure 6: Trapping region in the $(+, 0, -, -)$ boundary, for the network of Equation 17, projected onto a plane orthogonal to vector $(1, -1, -1)'$, with only the y_1 and y_4 components plotted (*i.e.*, x_1 and x_3 for $\mathbf{x} \in \mathbf{R}^3$), so the entire $(+, -, -)$ octant of $\mathbf{R}^3$ is projected onto the triangle with vertices $(0, 0)$, $(1, 0)$ and $(0, -1)$. The dotted lines define the (projected) returning cones for the five cycles, which partition the octant: marked by the letters A to E. The solid lines show projections of the images of the returning cones under their respective mappings. The image of the B region is the leftmost triangle. The image of the A region is the narrow triangle connected to the B region image. The narrow region separated from these comprises the images of the C, D and E regions, where the E region maps to the short lower piece, the D region maps to the upper part of the longer piece, not extending into the returning cone for B and the C region maps to the rest of the longer piece, intersecting all 5 returning cones. We take our trapping region to be the union of the images of the B, C, D and E regions as well as the part of the image of the A region that lies in the B region. The dashed region at top shows the extent to which the invariant cone of the next figure encroaches into this octant.

Figure 7: Invariant cone for the seven matrices in the Poincaré maps for the network of Equation 17, projected onto the unit sphere, indicated by solid lines. Projections of the invariant subspaces through eigenvectors are indicated by dashed lines.

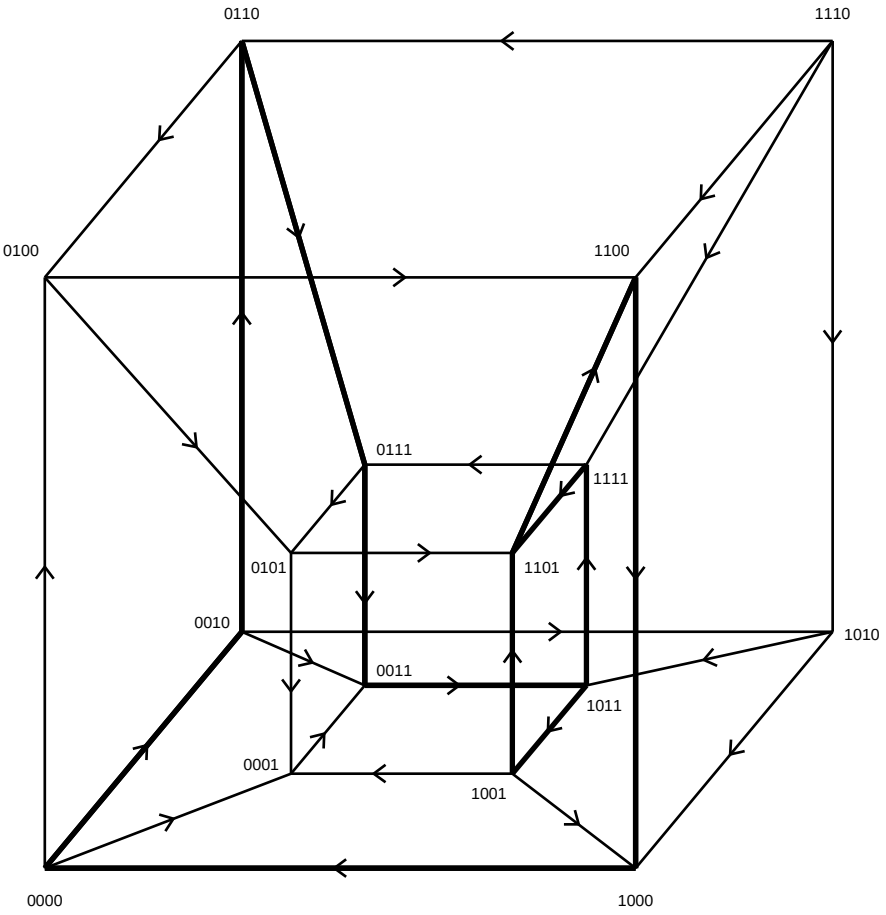

Figure 1, Edwards, DEDS

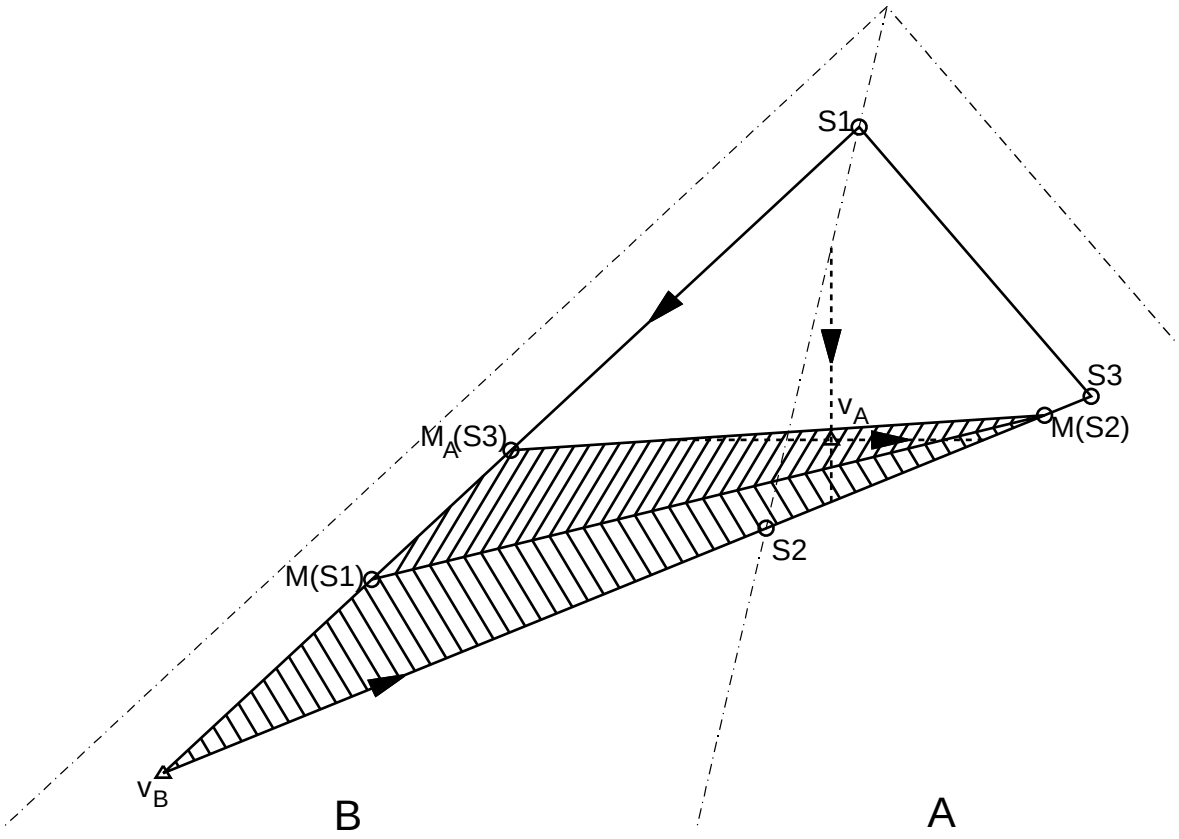

Figure 2, Edwards, DEDS

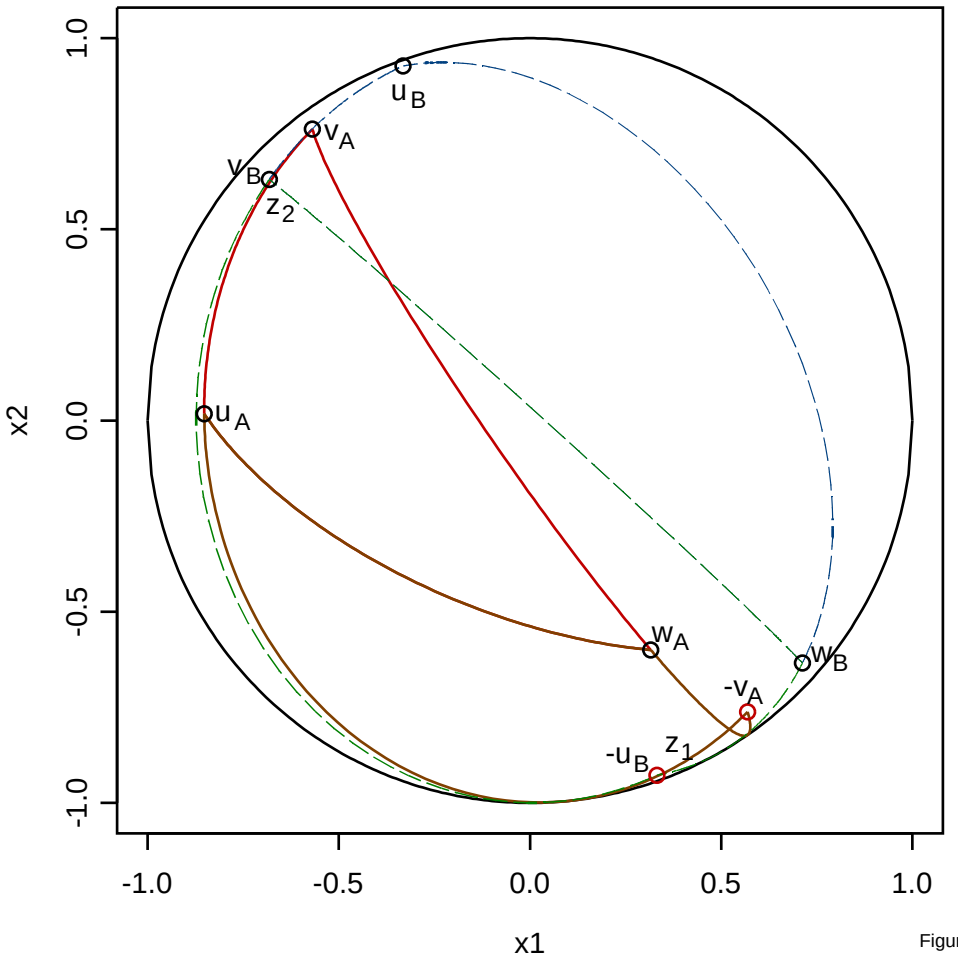

Figure 3, Edwards, DEDS

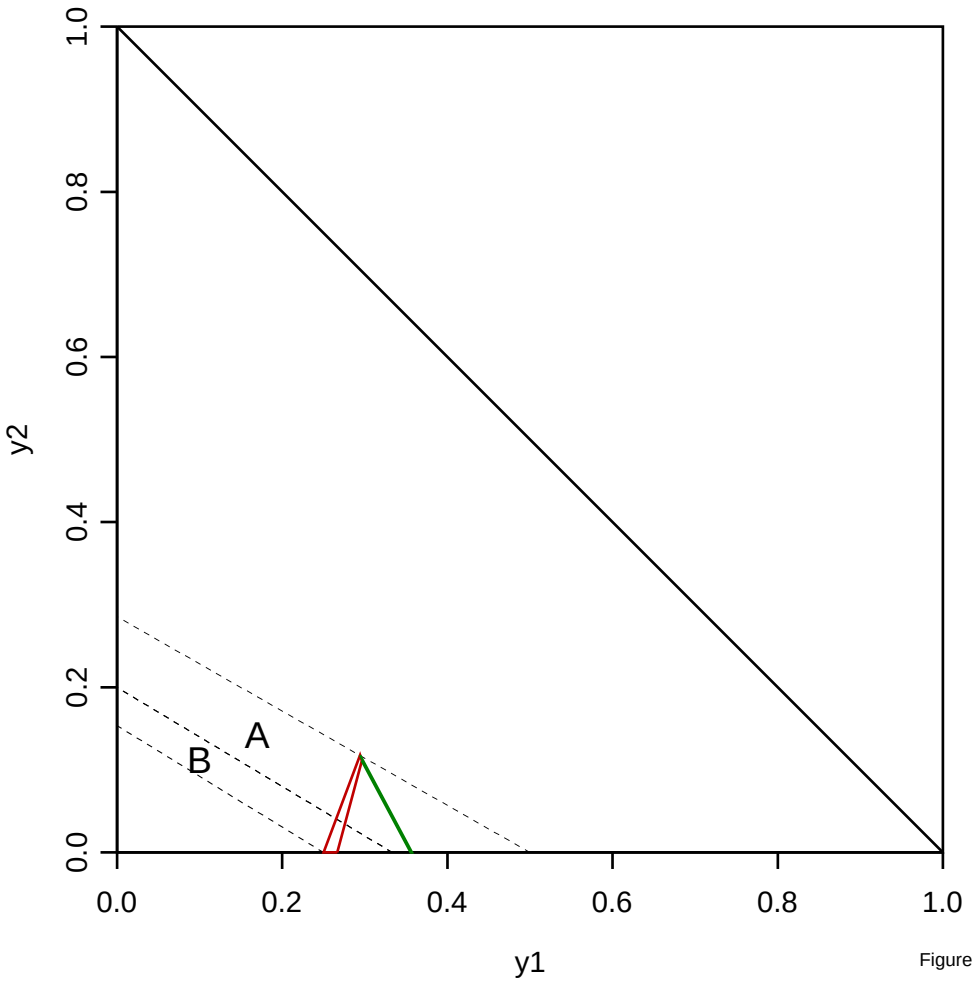

Figure 4, Edwards, DEDS

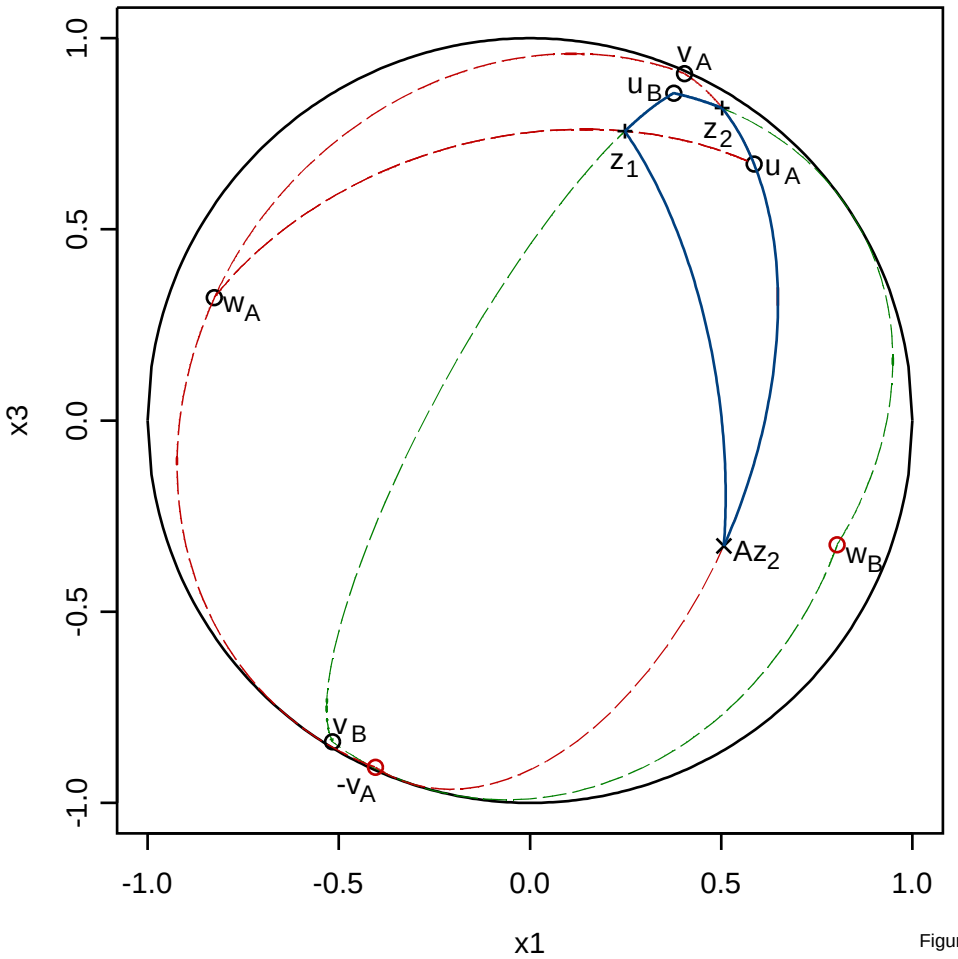

Figure 5, Edwards, DEDS

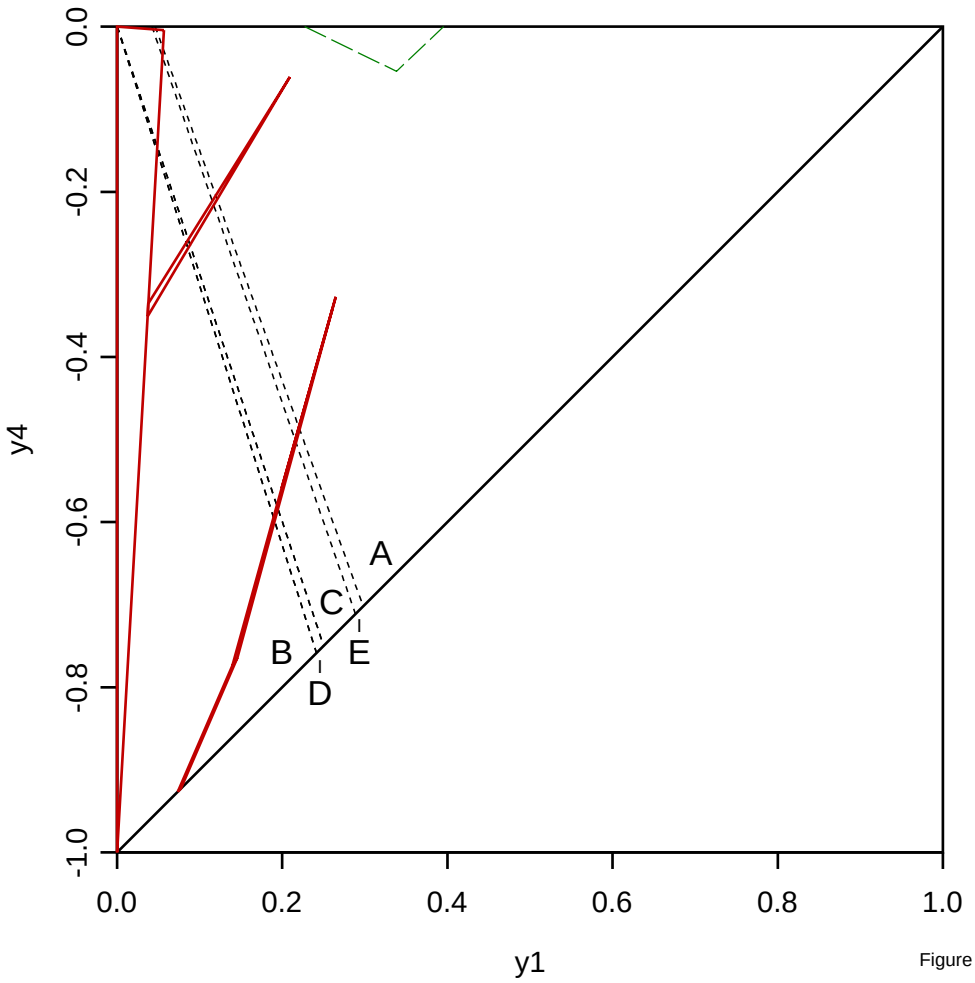

Figure 6, Edwards, DEDS

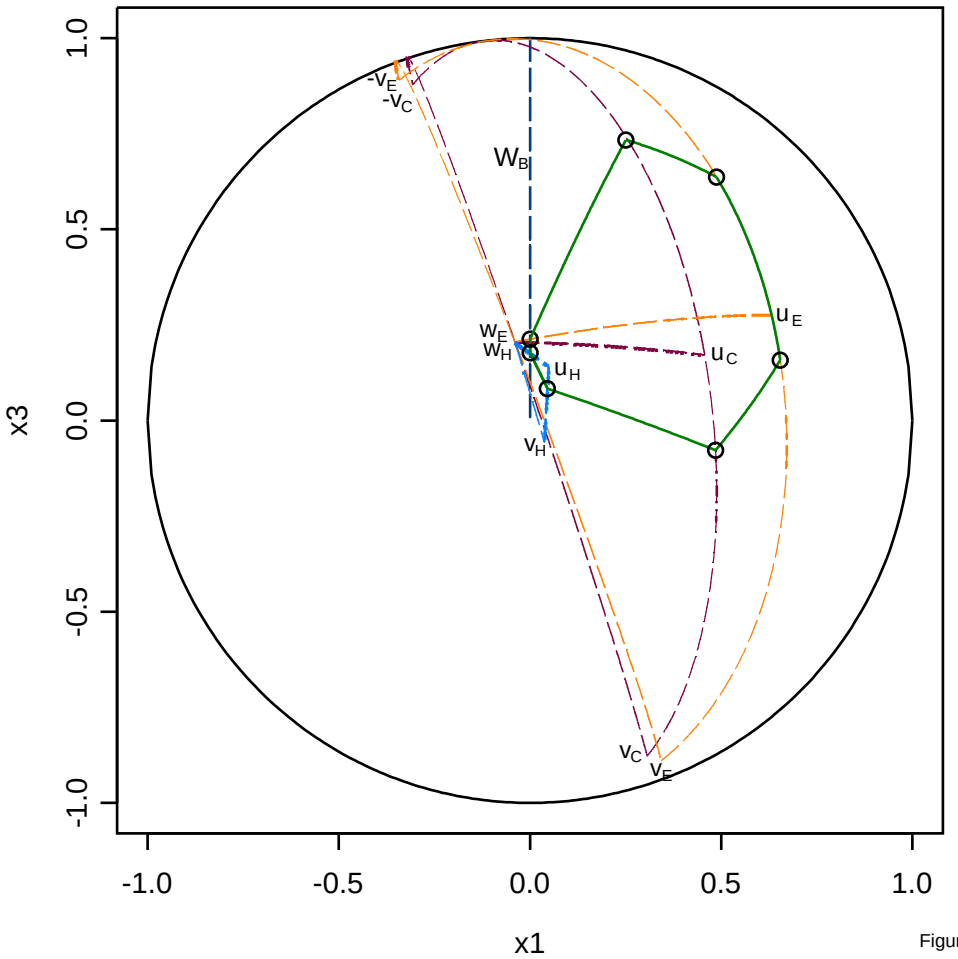

Figure 7, Edwards, DEDS